

Polystyrene/Organoclay Nanocomposites as Anticorrosive Coatings of C-Steel

L. A. Al Juhaiman^{}, D. A. Al-Enezi, W. K. Mekhamer*

Chemistry Department, King Saud University, Riyadh, Saudi Arabia

*E-mail: ljuhiman@ksu.edu.sa

Received: 7 April 2016 / Accepted: 3 May 2016 / Published: 4 June 2016

In the first part of this study, polystyrene/organoclay nanocomposites (PCN) were successfully prepared at different weight percentages of organoclay (OC) and were labelled 1-10% NC. This study investigates the use of these nanocomposites as anticorrosive coatings for C-steel in a 3.5% NaCl solution. Testing the anticorrosive properties of these nanocomposites was performed using the open circuit potential, Tafel method and electrochemical impedance spectroscopy. The 3% NC was observed to provide excellent corrosion protection and best film adhesion. Calculation of water permeation showed that the 3% NC also showed a much lower water absorption compared with that reported in other studies.

Keywords: Nanocomposite; C-steel; Film Adhesion; Electrochemical Impedance; Tafel; Water Permeation.

1. INTRODUCTION

Clay is one of the best green natural materials that can be used in many aspects of industry [1-22]. Recently, polymer–clay nanocomposites (PCNs) have gained interest in science and engineering owing to their unique physical, chemical and physicochemical properties compared with polymers or conventional composites. These properties include increased strength, decreased gas permeability, increased solvent and heat resistance and decreased flammability [3-12]. Applications include food packaging, anticorrosive coatings, microelectronics and biotechnology. PCNs are a new class of materials obtained by the dispersion of a few weight percent of clay (2:1 layered silicates) in the nanometer scale within the polymer matrix [3-12, 15-22]. Usually, PCNs are prepared by three methods: solution blending, in-situ polymerization and melt intercalation. Depending on the strength of the interfacial interactions between the polymer matrices and the layered silicates, the structures of

the PCNs are classified into intercalated, flocculated and exfoliated nanocomposites [3-12, 15-22]. The organoclay with lowered surface energies are more compatible with polymers and polymeric molecules and can intercalate within their interlayer space or galleries under well-defined experimental conditions [3-12].

Although there have been many studies on the synthesis of PCNs, most of the previous studies used pretreated clay (obtained from the market) in the preparation of the PCNs [3-12, 17-22], and a few studies modified the local clay [16, 23]. The preparation of PCNs with a good dispersion of clay layers within the polymer matrix is difficult simply by physical mixing of the polymer and clay particles owing to the high face-to-face stacking of clay layers. The intrinsic incompatibility of hydrophilic clay layers with hydrophobic polymer chains prevents the dispersion of the clay within the polymer matrix and results in weak interfacial interactions. Modification of the clay layers with a cationic surfactant to obtain the organoclay is necessary to render the clay layers more compatible with the polymer chains. Corrosion protection plays a prominent role in the modern metallic industry. Therefore, many organic–polymeric coatings have been employed to protect metals against corrosion. The mechanism for enhanced corrosion protection has been attributed to the increases in the corrosion potential and the length of the diffusion pathways for reactive gases, such as oxygen and water vapor, in the polymer coatings [24-29]. This leads to an enhancement of the corrosion protection of metallic substrates as compared with that of the neat polymer coating. The most direct way to determine the water content in a coating is by weight measurements, either as weight gain during absorption or as weight loss during drying. Other possible techniques include differential scanning calorimetry (detects only the clustered water), or by electrochemical impedance spectroscopy (EIS). The frequency of the AC potential perturbation ranged from 100 kHz to 100 mHz, thus allowing a new spectrum to be collected every 15 minutes. This acquisition rate was considered to deliver sufficient data for a detailed description of the water uptake process to be obtained [26].

Water permeation in a coating increases its polarity which is reflected by an increase in the capacitance of the coating. Hence, the water content can be determined by the electrochemical impedance method based on the fact that the presence of water increases the capacitance of the coating.

Polystyrene is an inexpensive polymer per unit weight. It is a poor barrier to oxygen and water vapor, which is necessary for the preparation of anticorrosive coating films. Some researchers have successfully used PS to prepare PS–clay hybrid nanocomposite materials using different methods or different clay compositions [3, 4, 17, 18, 23]. The main aim of the present study is to investigate the anticorrosive properties of PS/OC nanocomposite coatings, prepared in the first part of this study, and apply them on C-steel in 3.5% NaCl. Cross-cut testing for film adhesion on C-steel is applied. Moreover the anticorrosive properties of PS/OC nanocomposite coatings are investigated by electrochemical methods (open circuit potential, Tafel plots and electrochemical impedance spectroscopy).

2. EXPERIMENTAL METHODS

2.1. Materials

Polystyrene (PS) was purchased from Sabic Company, Kingdom Saudi Arabia, ($M = 259,000$ g/mol). Cetylpyridinium chloride (CPC, $(C_{21}H_{38}ClN \cdot H_2O)$ $M = 358.01$ g/mol) with a purity of 98% was provided by BDH, and was used as a cationic surfactant. Toluene, with 99.5% purity, was used as a solvent (Avonchem Co.). Sodium chloride (BDH) was used to prepare 3.5% w/w corrosive solution. The C-steel (CS) specimens were commercial rods (grade 1,046; ODS company, Germany). The chemical composition of CS is: C = 0.46%, Si = 0.18%, P = 0.013%, S = 0.006%, Cr = 0.18%, Cu = 0.03%, Al = 0.023% and the balance was iron. A CS rod was mounted in a glass tube of the appropriate diameter using epoxy resin to ensure that a constant cross-sectional area would be exposed to the solution.

2.2. Methods

2.2.1. Preparation of PS/OC nanocomposites

In the first part of this work (in press), the organic-modified clay (OC) was prepared by a cation-exchange reaction between the sodium cations of sodium clay (NaC) and cetylpyridinium chloride cations. The preparation of the PCN is illustrated in the first part of this investigation [23].

2.2.2. Coating the C-steel surface

C-steel rod samples were used as the working electrodes. The surface of the working electrode was polished with a polishing machine (Metaserve 2000) using emery papers with different grades (100, 220, 400, 1000). The C-steel rods were washed thoroughly with distilled water then immersed in acetone for 2 min in an ultrasonic cleaner. The PS in toluene/or PS/OC in toluene solutions were casted dropwise onto the C-steel rods then left in a fume hood for 2 hours. The prepared PCN at different wt% of organoclay were labeled 1% NC, 3% NC, 5% NC and 10% NC. The samples were dried in the oven overnight at 60 °C to provide coatings of approximately 95 ± 5 μm thickness, as measured by a coating thickness gauge (Elcometer 465). This method ensured a smooth coating with no bubbles.

2.2.3. Adhesion test

The adhesion test was performed on the coated C-steel samples using a cross hatch cutter instrument (Sheen Instruments, U.K.). A cross hatch pattern was made through the film to the C-steel substrate. Pressure-sensitive tape was applied over the cross hatch cut then the tape was removed by pulling it off as close to an angle of 180° as possible. Adhesion was assessed on a zero to five scale.

The adhesion using the cross-cut (cross hatch) testing for coating adhesion was performed according to ASTM D-3359-02.

2.2.4. Electrochemical methods

Open circuit potential, electrochemical impedance spectroscopy (EIS) and Tafel method were performed on a potentiostat/galvanostat (ACM Instruments, UK). A three electrode cell was used: C-steel rod as the working electrode with an exposed area of 9.35 cm^2 , a platinum auxiliary electrode, and a saturated calomel electrode (SCE) as the reference electrode. All electrochemical tests were performed and repeated in triplicate to ensure reproducible results. The corrosive medium was 3.5 wt% aqueous NaCl and the temperature was maintained at $30 \text{ }^\circ\text{C}$ using a water bath. The open circuit potential was recorded for one hour against the SCE reference electrode without applying an external potential until a constant potential was obtained (E_{corr}). Impedance measurements were performed in the frequency range of 100 kHz to 100 mHz. Tafel plots were obtained by scanning the potential $\pm 250 \text{ mV}$ from E_{corr} at a scan rate of 60 mV/min . Corrosion current density (I_{corr}) was determined through superimposing a straight line along the linear portion of the cathodic or anodic curve and extrapolation through E_{corr} .

The water content can be determined by electrochemical impedance method based on the fact that the presence of water increases the coating capacitance. In the present study, the change of coating capacitance with time from Nyquist results was used to calculate water permeation for 3% NC only.

3. RESULTS AND DISCUSSION

3.1. Adhesion test

Herein, the C-steel was coated with the pure PS and PS/OC films at a thickness of approximately $90\text{--}100 \text{ }\mu\text{m}$. The thicknesses of the PCN reported in the literature vary between $370 \text{ }\mu\text{m}$, by Yeh et al. [15], and $8.5 \text{ }\mu\text{m}$, by Kumar et al. [22]. The adhesion using the crosscut (cross hatch) testing for coating PS and 1–10 % OC were determined. The results showed that for the PS, 1% and 5% NC coatings, the area removed was 35–65%. However for 3% and 10% NC, none of the coating area was removed. Thus 3% and 10% NCs provided the best coating adhesion. This improvement in adhesion indicates that the prepared PCN filled the voids and crevices on C-steel [10], as shown in Table 1. In another study, Navarchian et al. obtained the best adhesion on a steel surface using the 3% clay of the polyaniline–clay nanocomposite [19]. However, Heidarian et al. [10] showed that 1% NC exhibited better adhesion than 3% NC on a steel surface using a polyurethane/organoclay nanocomposite.

Table 1. The adhesion parameters and the % area removed.

Sample Code	Adhesion Parameters	Area removed %
PS	1B	35-65%
1%NC	1B	35-65%
3%NC	5B	0%
10%NC	5B	0%

3.2. Electrochemical measurements

3.2.1. Open circuit potential

All electrochemical measurements were performed in 3.5% NaCl aggressive solution at 30 ± 1 °C. The values of the open circuit potential were recorded for one hour of immersion until the potential reached a steady state value (E_{corr}). The results are shown in the second column of Table 2. The corrosion potential (E_{corr}) of all coated samples was much higher than the E_{corr} of C-steel uncoated sample (bare), which agrees with previous studies [7–19]. Moreover, comparison of the E_{corr} of PCN-coated samples with that of the neat polymer (PS) showed that the 3% and 5% NCs had a much larger value (200 mV higher) than that of C-steel coated with PS or any other coating. However, E_{corr} of 1% and 10% NC is slightly higher than that of PS but higher than that of the uncoated samples.

3.2.2. Electrochemical impedance spectroscopy (EIS)

Electrochemical impedance spectroscopy (EIS) is a powerful technique in corrosion protection as it provides an accurate in situ method for characterizing polymer-coated metals and the changes in their performance during exposure to corrosive environments [25]. A ratio $A/d > 10^4$ centimeter provides satisfactory results, as suggested by Mansfield and co-workers who used an area (A) of 20 cm^2 for coating thicknesses, (d) of 10–50 μm [25]. In the present study, the ratio of $A/d = 10^5$ cm.

The Nyquist diagrams derived from the EIS measurements for all uncoated and coated C-steel samples exhibited the same behavior; all plots have semicircle shape which agrees with previous reports [10, 20]. The Nyquist plots of 1–10% NC coated C-steel electrodes measured at 30 °C in 3.5 wt% NaCl solution are shown in Figure 1.

The semicircle of uncoated C-steel and that for C-steel coated with PS are not shown, as the semicircles are much smaller than those observed for the samples coated with PCN indicating that PS exhibits a much lower impedance value than PCN coated C-steel. The EIS parameters are shown in Table 2. The impedance values (R) are higher for the coated samples, which is in agreement with many previous studies [10, 15, 20]. The R values increased from 6.91×10^2 Ohm. cm^2 for the bare C-steel to

$4.72 \times 10^8 \text{ Ohm.cm}^2$ for 3% NC then decreased with increasing clay content. This behavior indicated an improved corrosion protection of the steel substrate.

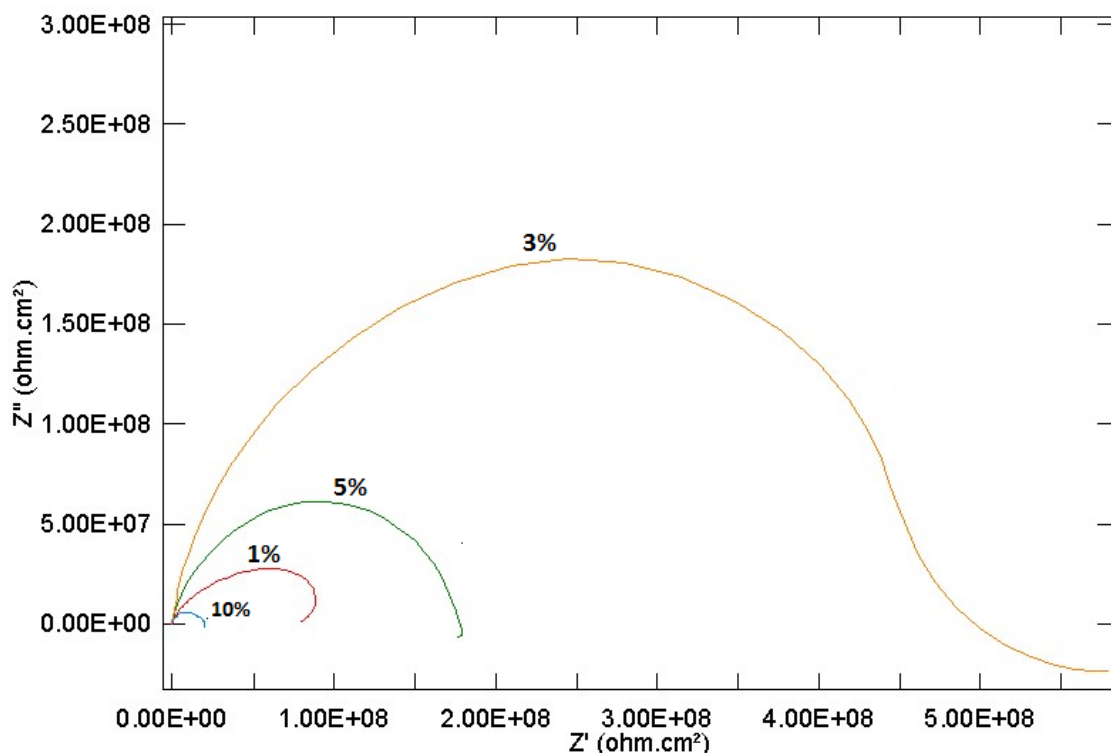


Figure 1. Nyquist plots for 1-10% NC.

Thus 3% NC provided the best coating. Huang et al. [12] obtained the best corrosion protection in preparing a series of polyimide–clay nanocomposite (PCN) materials for cold rolled steel at 3 % [12]. Other reports showed that a 5% waterborne polyurethane sodium montmorillonite (Na^+ -MMT) clay nanocomposite was the best formulation for polyimide–clay nanocomposite (PCN) materials [15]. Thus the incorporation of a small amount of OC into the PS coating greatly increased the impedance R and reduced the coating capacitance C relative to pure PS[12,15].

Table 2. EIS parameters for bare steel, PS and PCN coating at 30° C in 3.5 wt% NaCl.

Sample	EIS parameters		
	E_{corr} (mV)	R (Ohm.cm^2)	C (F/cm^2)
Bare	-569	6.91×10^2	9.27×10^{-6}
PS	-488	1.004×10^6	8.298×10^{-7}
1%NC	-499	8.002×10^7	2.62×10^{-10}
3%NC	-281	4.72×10^8	1.396×10^{-10}
5%NC	-244	1.783×10^8	2.84×10^{-10}
10%NC	-499	1.961×10^7	6.46×10^{-10}

3.2.3. Tafel method

The Tafel method was applied, and Tafel constants were calculated from a slope at ± 50 mV with respect to E_{corr} using a computational least-squares analysis. The corrosion current density i_{corr} , which is equivalent to the corrosion rate, is given by the intersection of the extrapolation of the Tafel lines. It is known that i_{corr} values presents a kinetic characteristic of a given metal-electrolyte system Tafel plots for bare, PS and 1–10% NC coated C-steel electrodes measured at 30 °C are shown in Figure 2.

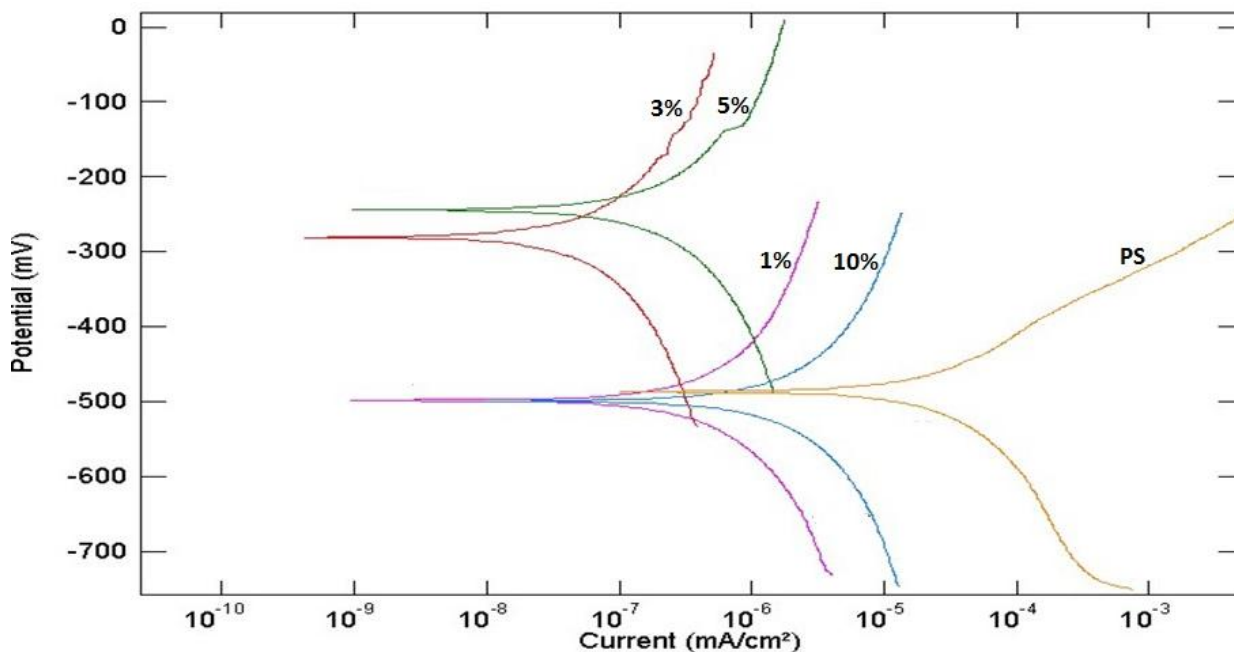


Figure 2. Tafel plots for PS and for 1-10% NC.

Table 3. Tafel parameters for bare steel, PS and PCN coating at 30°C in 3.5 wt% NaCl.

Sample	Tafel Parameters			
	E_{corr} (mV)	i_{corr} (A/cm ²)	CR(mm/yr)	% Protection relative to PS coating
Bare	-569	5.42×10^{-5}	0.610
PS	-488	8.361×10^{-8}	9.56×10^{-4}
1%NC	-499	3.566×10^{-10}	4.08×10^{-6}	99.57%
3%NC	-281	4.798×10^{-11}	5.47×10^{-7}	99.94
5%NC	-244	1.746×10^{-10}	1.20×10^{-6}	99.87
10%NC	-499	1.56×10^{-9}	1.78×10^{-6}	99.81

The corrosion parameters calculated from the Tafel plots are summarized in Table 3. The i_{corr} values decreased from $5.42 \times 10^{-5} \text{ A/cm}^2$ for the bare C-steel to the lowest value of $4.798 \times 10^{-11} \text{ A/cm}^2$ for 3% NC, then increased slightly with increasing clay loading. The decrease of corrosion current density (or corrosion rate), as indicated in Table 3, arises from the incorporation of OC in the PS matrix that promotes the anticorrosive efficiency of the coated C-steel samples. This effect is enhanced as the clay loading is increased up to 3 wt% then decreases at high clay loading, which agrees well with previous studies [9, 20, 21]. Our results are in agreement with Olad et al. [11], Huang et al. [12] and Lai et al. [29] where a PCN film at 3% NC gave the best corrosion protection. However, the present results are opposite to those reported by Yeh et al. [4], who reported that as the clay loading increased from 1% to 10% clay loading, the corrosion protection increased.

Moreover, comparison of the protection efficiency or anticorrosive properties using polymer nanocomposite films in the present study with previous studies using other polymer/clay nanocomposites showed that the present PNC exhibited better corrosion protection in terms of current density values, as shown in Table 4.

Table 4. Comparison of the anticorrosive properties of our PCN with other studies.

Ref. No.	i_{corr} (A/cm ²)
Yeh et al.[4]	2.5×10^{-7}
Ahmad et al. [6]	6.50×10^{-9}
Piromruen et al. [9]	1.36×10^{-4}
Heidarian et al. [10]	1.39×10^{-10}
Olad and Rashidzadeh [11]	7.5×10^{-7}
Huang et al. [12]	1.09×10^{-6}
Navarchian et al. [21]	4.67×10^{-7}
Chang et al. [23]	1.28×10^{-6}
Present study	4.798×10^{-11}

3.3. Water permeation process

Fick's first law of diffusion expresses the rate of species diffusing into materials:

$$J = -D \delta c / \delta x \quad (1)$$

where D is the diffusion coefficient, J is the rate of transfer per unit area, C is the local concentration of water in the coating and x is the directional distance.

The water content can be determined by electrochemical impedance method based on the fact that the presence of water increases the coating capacitance. The two impedance components exhibit opposite trends with time, namely the coating resistance (R) continuously decreases, whereas the coating capacitance increases with time. If the coating is treated as a parallel plate capacitor, then its capacitance is related to the dielectric constant ϵ by the famous relation:

$$C = \epsilon \epsilon^{\circ} A / d \quad (2)$$

where ϵ_0 is the dielectric constant of free space (8.854×10^{-14} F/cm), A is the surface area of the coating and d is the coating thickness. The relative dielectric constant of polymers is typically in the range of 3–8, and that for pure water is 78.3 at 25 °C. The uptake of water will lead to a rise in the permittivity, resulting in a higher capacitance. The increase of coating capacitance with time occurs at a faster rate upon immersion in the aggressive electrolyte, and progressively slows until a saturation stage is attained at a sufficiently long time [26]. In the present study, the effect of immersion time was studied by Nyquist method for 3% NC only, as shown in *Table 5*. It was observed that C values increased after 12 hours and reached a constant value of approximately 3.53×10^{-10} F/cm² after 36 hours. This minor increase in the coating capacitance arises from the water absorption, which reached a maximum after 36 hours. The percentage of water uptake values may be calculated using different models. The most famous model is the Brasher–Kingsbury (BK) model, which was first introduced in 1954 and shown by the following equation:

$$\% \text{ Water uptake} = \log (C_t/C_0) / \log 80 \quad (3)$$

where C_t and C_0 are the electrical capacitance of the coating during and before the immersion. C_0 was calculated from extrapolating the graph of C_t with time and 80 is the dielectric constant of water.

Applying Eq. (5) is presented in Figure 3, where the water uptake reached a constant value of 0.228% after 36 hours (2160 minutes), whereas the saturation stage was reached after 22 hours (1300 minutes) for Moreno et al. [26]. Dolatzadeh et al. [27], using EIS, applied the BK model to study the effect of nano silica on the moisture absorption of polyurethane clear coats. They obtained 2.8–3.6% water uptake after 3600 min [27]. Moreno et al. [26] applied the BK model using different organic coatings for steel and the % of water uptake ranged between 6–9% after 2000 minutes, while in the present study, water uptake was only 0.23% after 2160 minutes (36 hours) and remained constant for approximately 48 hours. For the study by Castella et al. [28] using the BK model, the % water uptake after 6000 min was approximately 27% for a poly vinyl chloride coating; 3.25% water uptake for a polyester coating and 3.75% water uptake for poly vinylidene fluoride coating. The low value of water uptake in the present formulation may explain their good anticorrosive properties.

Table 5. Effect of immersion time on Nyquist parameters for NC coating at 30°C in 3.5 wt% NaCl

Time of immersion(h)	R (Ohm.cm ²)	C (F/cm ²)
1h	4.720×10^8	1.396×10^{-10}
12h	1.067×10^8	2.519×10^{-10}
24h	1.390×10^7	2.790×10^{-10}
36h	5.297×10^6	3.530×10^{-10}
48h	2.763×10^6	3.557×10^{-10}

There are no definite rules that regulate the coating thickness. Thicker films should allow greater amounts of water to be absorbed leading to smaller capacitance values [26]. This difference between the present results and those reported by Moreno et al. [26] may arise from the coating materials and the coating thickness. The thickness of the coating in the present study is $95 \pm 5 \mu\text{m}$ while that of Moreno et al. [26] ranged from 60–244 μm .

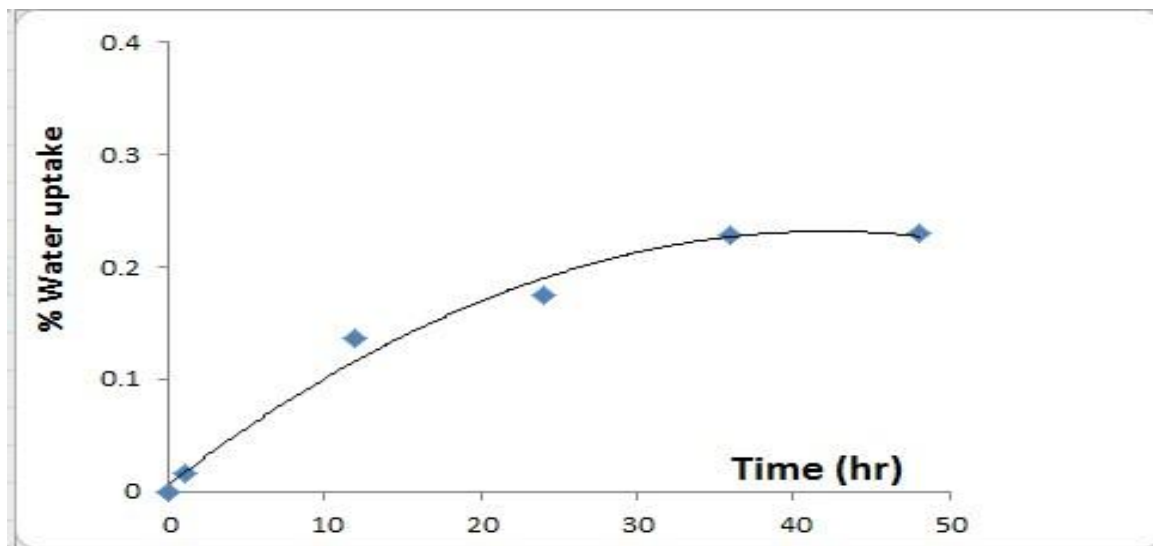
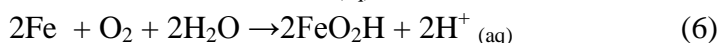
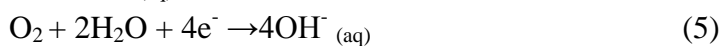


Figure 3. The change of % water uptake with time for 3% NC.

3.4. Corrosion Protection mechanism

The corrosion and rust formation on a steel surface may involve several steps of oxidation and reduction equations as shown below:



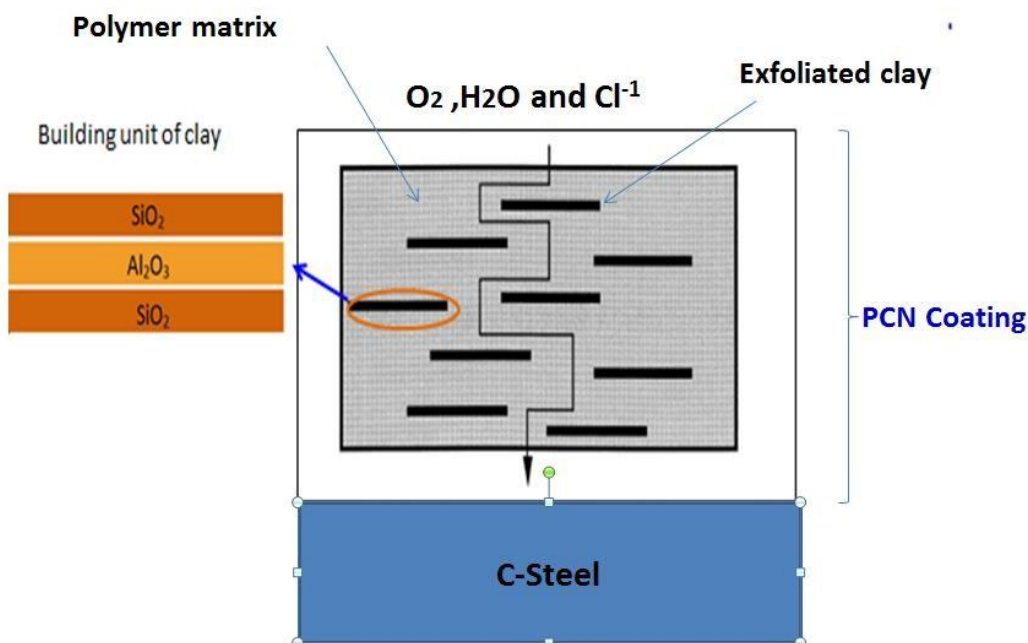
It could be observed that for corrosion to occur there is a need for sufficient H_2O and O_2 to enable the formation of rust and dissolution of the steel. The diffusion of pollutants across the coating surface is the beginning of the corrosion process. In the presence of Cl^- ions, the substitution of water molecules on the C steel surface with Cl^- ions leads to the probability of rapid rusting of the C-steel surface. If any of these processes are prevented, the corrosion is inhibited and the coating becomes effective for corrosion prevention. The enhanced corrosion protection may result from the dispersion of silicate nano layers in the PS matrix which increases the tortuosity of the diffusion pathway of the corrosive agents, such as oxygen, Cl^- ions and water [4, 9, 21].

The electrochemical corrosion reaction may occur at the areas of poor adherence between the polymer or polymer/clay film and the steel surface leading to the formation of corrosion products below the surface and induces swelling of the steel below the film surface. Corrosion protection is provided by these coatings by forming an efficient barrier to corrosive agents (chloride ions, water and

oxygen) that effectively separate the anode from the cathode, electrically [24, 29]. The enhancement of anticorrosion arose from the fact that the inorganic clay, with a plate-like shape and high-aspect ratio, is able to effectively extend the diffusion pathways of O₂, H₂O and Cl⁻ across the PCN, as well as to decrease the permeability of the coating. The model of diffusion pathways extension can be explained by the following equation of Nielsen proposed in 1967:

$$d' = d + (dLV_f / 2W) \tag{9}$$

where *d* is the ideal thickness of the coating, *L* is the mean length of silicate layers, *W* is the mean thickness of silicate layers and *V_f* is the silicate layers' volume fraction of the nanocomposites. The mean diffusion pathways of gas and liquid molecules are given by *d'*. Based on the results of TEM and XRD of the present formulations in the first part of this work [23], the silicate nanolayers of clay dispersed in the polymer matrix increased the tortuosity of the diffusion pathway for the corrosive agents. The high values of impedance from Table 2 and the high percentage of corrosion protection in Tables 3 which range between 99.5-99.9% are in agreement with the results of % water permeation. The results of % water permeation in the present study showed that the water uptake was only 0.23% after 2160 minutes (36 hours) and remained constant for approximately 48 hours. This low absorption of water support the following proposed model of torturous diffusion path of PCN coating which is presented schematically in Scheme 1.



Scheme 1. Proposed model for the torturous diffusion path in C-steel coated with PCN

4. CONCLUSION

In the first part of this study, a series of PS–clay nanocomposite materials was prepared by the surface modification of raw Khulays clay from the western region of Saudi Arabia. The as-synthesized nanocomposite materials were characterized by FTIR, XRD and TEM, which confirmed the existence

of the organoclay in the polymer matrix. XRD and TEM proved the exfoliated structure was obtained for the low clay loading (1–5% NC) while 10% NC showed an intercalated structure.

In the present study, the prepared PCN are used to prepare eco-friendly coatings for C-steel in 3.5% NaCl solutions. Cross-cut testing for film adhesion showed that nanocomposite films at 3% and 10% NC exhibited the best adhesion. The higher corrosion resistance performance of PCN compared with PS indicates that the incorporation of silicate nanolayers of clay in the matrix of PS considerably enhances the corrosion protective performance of the coatings. It is also observed that the extent of protection provided by PCN coatings depends upon the loading of the clay. Among the coated specimens, 3% NC offers the best corrosion protection performance based on the EIS and Tafel results. The effect of immersion time was studied by the EIS method and showed that the % water uptake was very low and reached a constant value of 0.223% after 36 hours. The water uptake in the present study, computed from the capacitance data, was much lower than most of the previously reported data. Based on the Tafel method, 3% NC coating on C-steel was found to exhibit the best anticorrosive properties compared with bulk PS or the other PCN. The enhanced corrosion protection of the nanocomposite films compared with the PS-coated samples, resulted from the dispersion of silicate nanolayers in the PS matrix that increased the tortuosity of the diffusion pathway for the corrosive agents. In conclusion, novel PCN materials made from a polymer and ecofriendly clay provide an effective method to protect metals against corrosion. Comparison of nanocomposite films at 3% NC coatings with other studies using other polymer–clay nanocomposite formulations showed that this coating gave better corrosion protection.

ACKNOWLEDGEMENT

The authors extend their appreciation to the Deanship of Scientific Research at King Saud University for funding the work through the research group project No. RGP-102. All authors do not have any conflicts of interest to declare.

List of symbols:

- PCN Polymer clay nanocomposites.
- NaC Sodium saturated clay.
- OC Organoclay prepared by a cation-exchange between sodium cations of NaC and cetylpyridinium chloride cations(surfactant).
- Ps Polystyrene.
- PS/OC Prepared at different content of OC (0, 1, 3, 5 & 10 wt %).
- E_{corr} Open circuit potential (mV).
- R Impedance value from Nyquist plot (Ohm.cm^2).
- C Capacitance of coating (F/cm^2).
- i_{corr} Current density (A/cm^2).
- d Ideal thickness of the coating(m).
- L The mean length of silicate layers (m).
- W Mean thickness of silicate layers (m).
- V_f The silicate layers' volume fraction of the nanocomposites.
- d' Mean diffusion pathways of gas and liquid molecules(m).
- C_0 Electrical capacitance of the coating before immersion in corrosive medium.
- C_t electrical capacitance of the coating during immersion in corrosive medium.

References

1. A. Tracton, Editor, *Coating Materials and Surface coatings*, CRC Press, New York (2006).
2. F. Bergaya, B. Theng and G. Lagaley, *Handbook of Clay Science*, Elsevier Publisher, Netherland (2006).
3. S. Qutubuddin, X. Fu and Y. Tajuddin, *Polym. Bull.*, 48, (2002)143.
4. J. M. Yeh, S.J. Liou, C.G. Lin, Y. P. Chang, Y.H. Yu and C.F. Cheng, *J. App. Polym. Sci.*, 92, (2004)1970.
5. R.A. Vaia and E.P. Giannelis, *Macromolecules*, 30, (1997)8000.
6. G. Lagaly, *Solid State Ionics*, 22, (1986)43.
7. D. Zaarei, A.A. Sarabi, F. Sharif and S.M. Kassiriha, *J. Coat. Technol. Res.*, 5, (2008)241.
8. S. Ahmad, F. Zafar, E. Sharmin, N. Garg and M. Kashif, *Prog. Org. Coat.*, 73, (2012)112.
9. P. Piromruen, S. Kongparakul and P. Prasassarakich, *Prog. Org. Coat.*, 77, (2014)691.
10. M. Heidarian, M.R. Shishesaz, S.M. Kassiriha and M. Nematollahi, *Prog. Org. Coat.*, 68, (2010)180.
11. A. Olad and A. Rashidzadeh, *Prog. Org. Coat.*, 62, (2008)293.
12. H.Y. Huang, T.C. Huang, T.C. Yeh, C.Y. Tsai, C.L. Lai, M.H. Tsaib, J.M. Yeh and Y.C. Chou, *Polymer*, 52, (2011)2391.
13. W. K. Mekhamer, *J. Saudi Chem. Soc.*, 14, (2010)301.
14. M.H. Al-Qunaibit and L.A. Al Juhaiman, *Inter. J. Basic & App. Sci.*, 12, (2012)205.
15. J.M. Yeh, C.T. Yao, C.F. Hsieh, L.H. Lin, P.L. Chen, J.C. Wu, H.C. Yang and C.P. Wu, *Eur. Polym. J.*, 44, (2008)3046.
16. M. Alshabanat, A. Al-Arrash and W. Mekhamer, *J. Nanomater.* 2013(2013). Article ID 650725. Retrieved from: <http://dx.doi.org/10.1155/2013/650725>
17. P.K. Paul, S.A. Hussain and D. Bhattacharjee, M. Pal, *Bull. Mat. Sci.*, 36, (2013)361.
18. A. Giannakas, C.G. Spanos, N. Kourkoumelis, T. Vaimakis and A. Ladavos, *Eur. Polym. J.*, 44, (2008)3915.
19. A. Navarchian, M. Joulazadeh and F. Karimi, *Prog. Org. Coat.*, 77, (2014)347.
20. J.T. Zhang, J.M. Hu, J.Q. Zhang and C.N. Cao, *Prog. Org. Coat.*, 49, (2004)293.
21. K.C. Chang, S. T. Chen, H.F. Lin, C.Y. Lin, H.H. Huang, H.H. Yeh and Y.H. Yu, *Euro. Polym. J.*, 44, (2008)13.
22. A. M. Kumar and Z.M. Gasem, *Prog. Org. Coat.*, 70, (2015)387.
23. L.A. Al Juhaiman, D.A. Al-Enezi and W.K. Mekhamer, *Digest J. Nanomaterials Biostructures*, 11, (2016)105.
24. R. Zaidi-zang, A. Ershad-langroudi and A. Rahimi, *Prog. Org. Coat.*, 53, (2005)286.
25. F. Mansfield, *J. Appl. Electrochem.*, 25, (1995)187.
26. C. Moreno, S. Hernández, J.J. Santana, J. González-Guzmán, R.M. Souto and S. González, *Int. J. Electrochem. Sci.*, 7, (2012)8444.
27. F. Dolatzadeh, S. Moradian and M. M. Jalili, *Prog. Color Colorants Coat.*, 3, (2010) 92.
28. A.S. Castela and A.M. Simões, Assessment of water uptake in coil coatings by capacitance measurements, *Prog. Org. Coat.*, 46, (2003)55.
29. M. C. Lai, K.C Chang, J. M. Yeh, S. J. Liou, M.F. Hsiehc and H. S. Chang, *Euro. Polymer J.*, 43, (2007)4219.